a

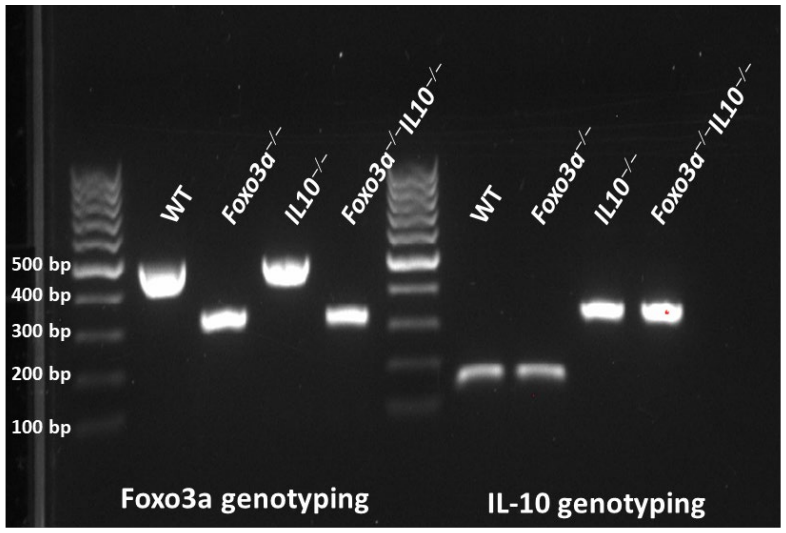

b

Frequency distribution of Foxo3a$^{+/-}$IL-10 $^{+/-}$ inter-cross			
Genotype	**% Expected Frequency**	**% Observed Frequency**	**# of mice**
Foxo3a$^{+/+}$ IL10 $^{+/+}$	6.25	8.06	20
Foxo3a$^{+/+}$ IL10 $^{+/-}$	12.5	9.27	23
Foxo3a$^{+/+}$ IL10 $^{-/-}$	6.25	5.24	13
Foxo3a$^{+/-}$ IL10 $^{+/+}$	12.5	14.51	36
Foxo3a$^{+/-}$ IL10 $^{+/-}$	25	29.03	72
Foxo3a$^{+/-}$ IL10 $^{-/-}$	12.5	14.51	36
Foxo3a$^{-/-}$ IL10 $^{+/+}$	6.25	5.24	13
Foxo3a$^{-/-}$ IL10 $^{+/-}$	12.5	7.66	19
Foxo3a$^{-/-}$ IL10 $^{-/-}$	6.25	6.45	16
Total	100	99.97	248

c

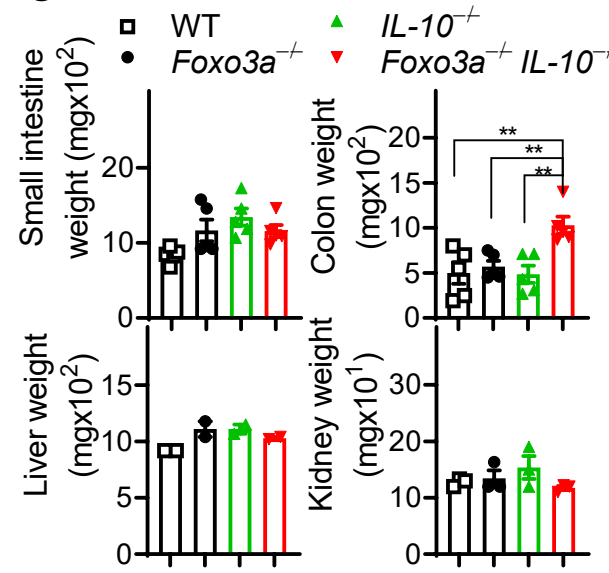

d

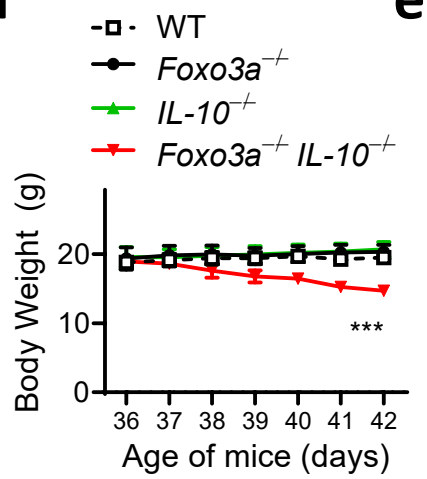

e

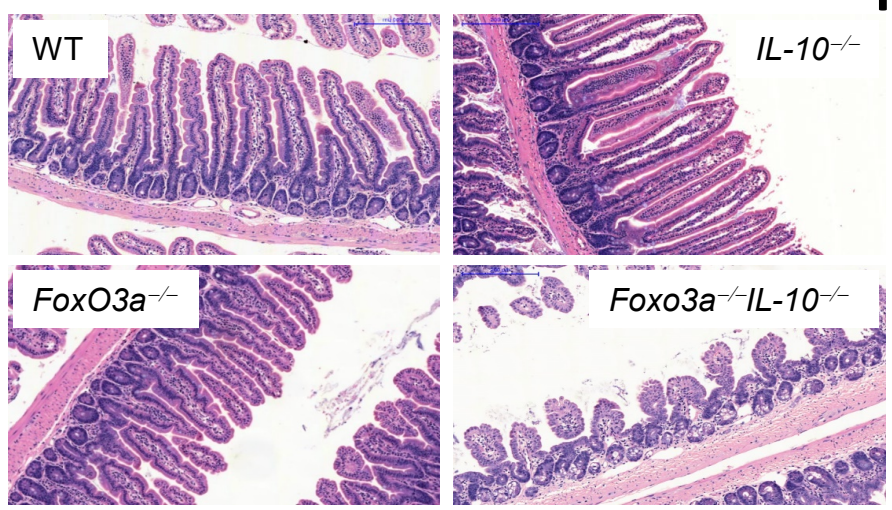

f

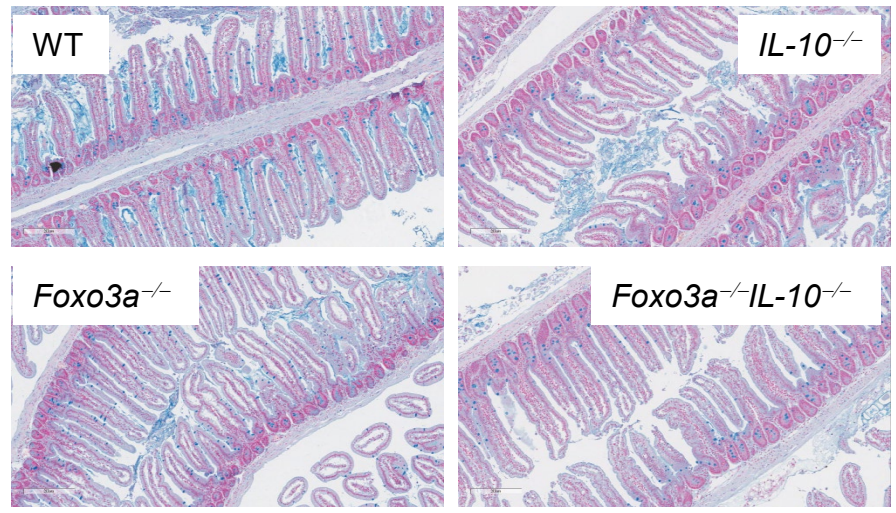

g

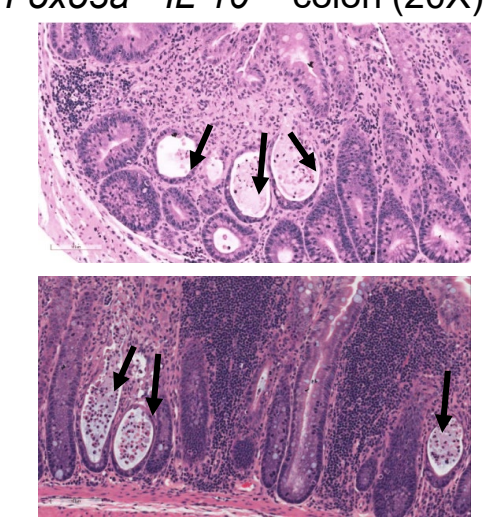

h

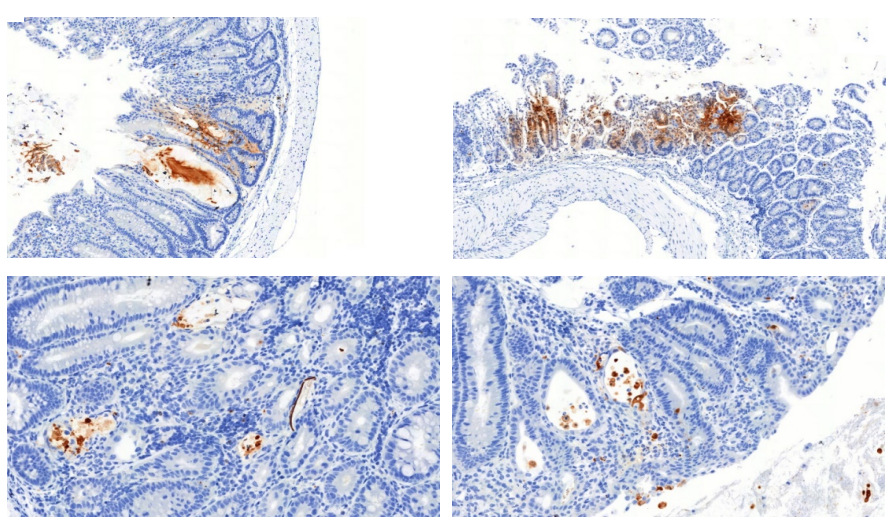

i

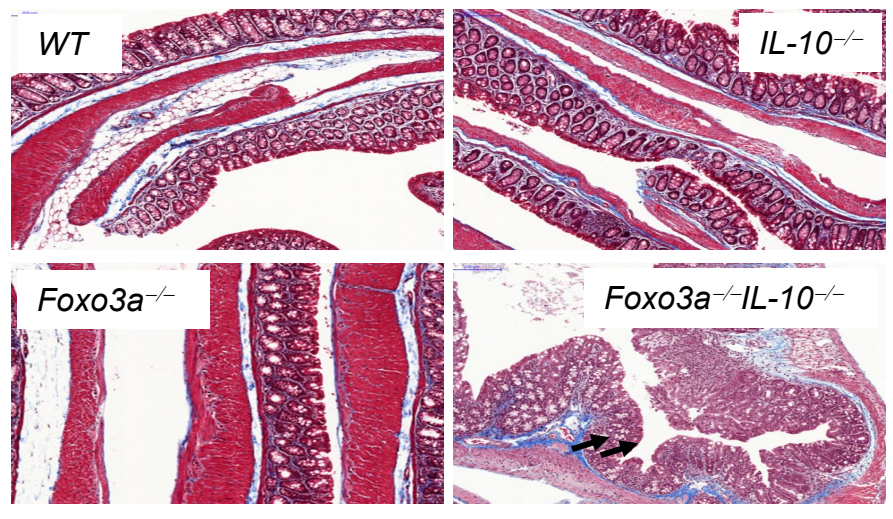

Fig. S1 Deficiency in Foxo3a leads to inflammatory lesions and apoptotic crypts in colons of *Il-10$^{-/-}$* mice. (**a**) Genotyping for Foxo3a and IL-10. (**b**) Frequencies of mice (n=248) born following *Foxo3a$^{+/-}$IL10$^{+/-}$* inter-cross. (**c**) Weights (mg) of different organs in the four groups of 6 weeks old mice.(**d**) Changes in body weight (grams) of mice prior to reaching humane endpoint (n=7). (**e**) Representative images (H&E) of the small intestines of the four groups of mice. (**f**) Representative images of Alcian blue staining of the small intestines of the four groups of mice. (**g**) Representative images (H&E) of the colons of *Foxo3a$^{+/-}$IL10$^{+/-}$* mice at 20x. Arrows indicate apoptotic crypts. (**h**) Representative images of the colons of *Foxo3a$^{+/-}$IL10$^{+/-}$* mice stained with anti-Caspase 3 antibody by IHC. (**i**) Representative images (Masson Trichrome staining) of the colons of the four groups at 10x. Arrows indicate areas of mild fibrosis. Data are representative of a minimum of three mice per group. One-way ANOVA was used to determine differences in body and organ weights. Data in panels **e-i** is from mice at 6 weeks after birth. Data represent the mean ±SEM (*P< 0.05, ***P<0.001 and ****P<0.0001).

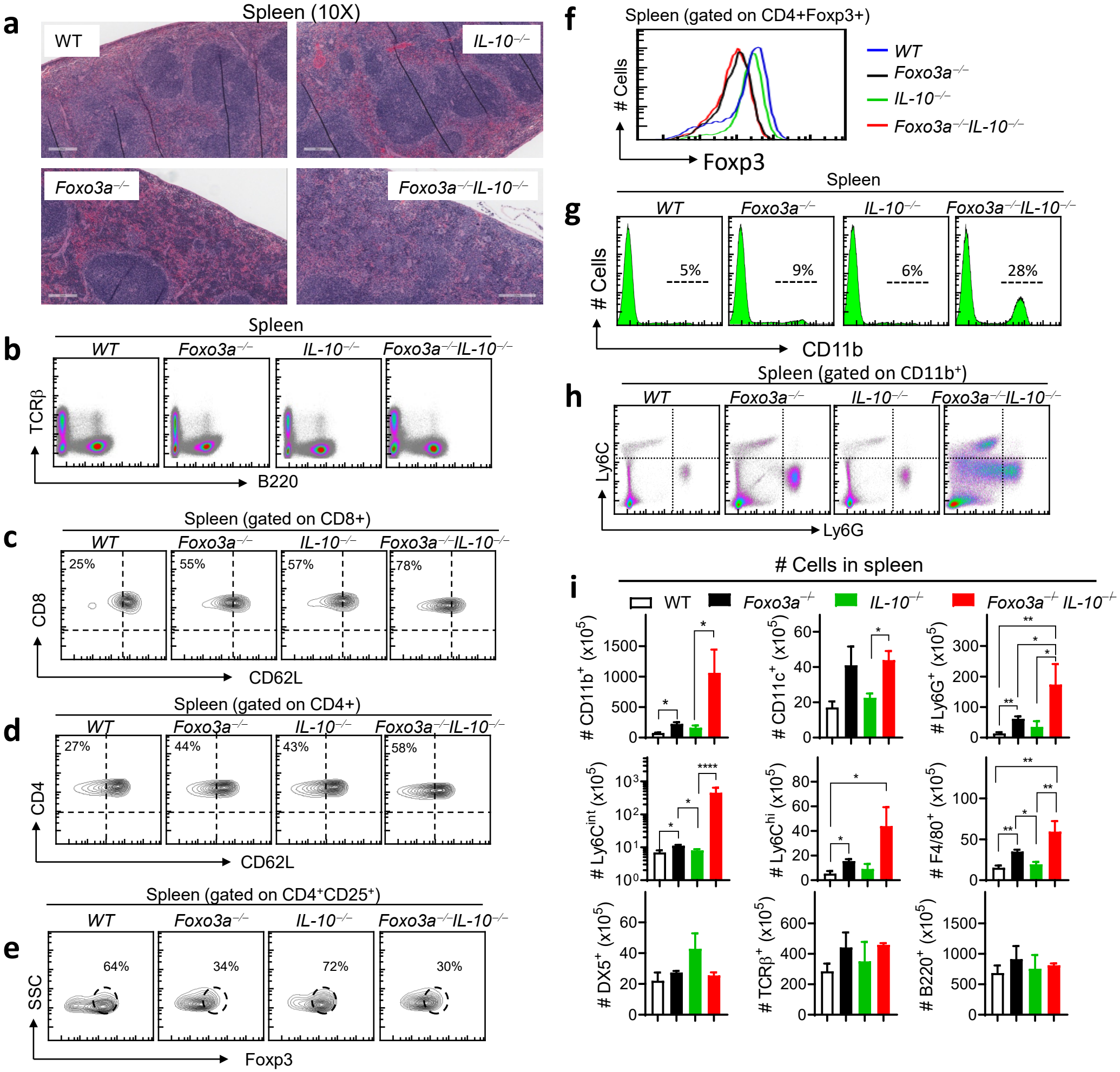

Fig. S2 Foxo3a controls the number and activation of peripheral immune cells. (**a**) Representative H&E images of the spleens of 8-week-old mice. (**b**) Representative FACS plots showing the T-cell and B-cell populations. (**c, d**) Representative FACS plots showing CD62L expression in splenic $CD4^+$ and $CD8^+$ T-cells of the four groups of mice. (**e**) Representative FACS plots showing SSC vs. Foxp3 expression in $CD4^+CD25^+$ cells in the spleens of the four groups of mice. (**f**) Representative histograms showing Foxp3 expression in splenic $CD4^+$ $FoxP3^+$ T-cells of the four groups of mice. (**g**) Representative histograms showing the percentage of $CD11b^+$ cells in the spleens of the four groups of mice. (**h**) Representative FACS plots showing the distribution of monocytes and neutrophils in the spleens of the four groups of mice. (**i**) Total numbers of myeloid and lymphoid cell subsets in the spleens of the four groups of mice. Data are representative of a minimum of three biological replicates per group. Graphs depict mean ±S.E.M. Statistics were done using One-way ANOVA (*P< 0.05, ***P<0.001 and ****P<0.0001).

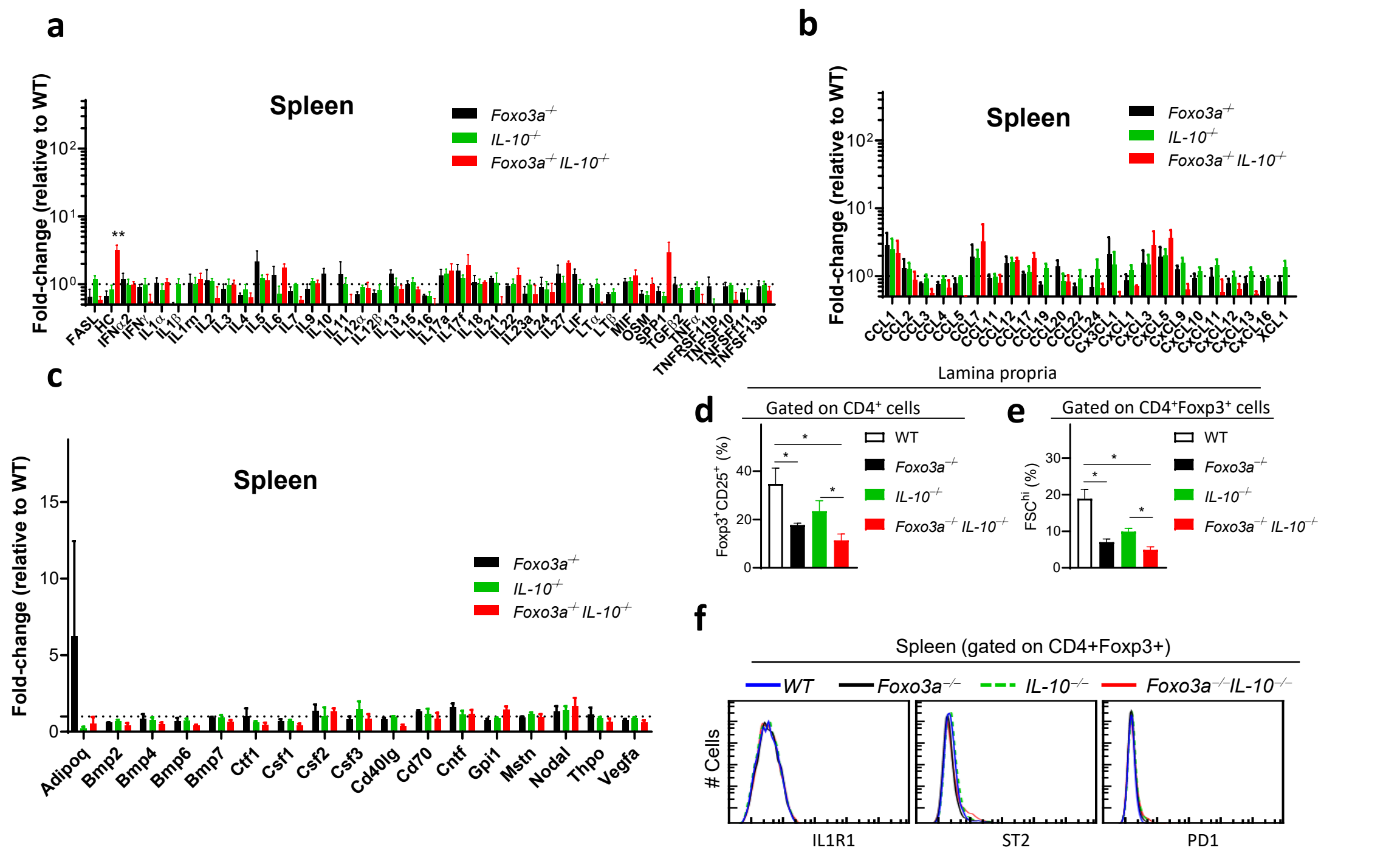

Fig. S3 Foxo3a deficiency does not impact the inflammatory profile of cells in naïve spleens of *IL-10* -deficient mice.

(**a-c**) Expression of inflammatory cytokines and chemokines in the spleens of the four groups of naïve mice measured by q-RT PCR (RT2 profiler array). Data are representative of four biological replicates per group, each being an average of 2 experimental replicates. (**d, e**) Quantitation of data shown in Fig. **3e** and **3f** respectively. (**f**) Representative histograms showing the expressions of IL-1R1, PD-1 and ST2 in splenic $CD4^+$ $Foxp3^+$ T-cells. Data are representative of three biological replicates per group (**d-f**). All graphs depict mean ±SEM. Statistics were done using One-way ANOVA (*P< 0.05, ***P<0.001 and ****P<0.0001).

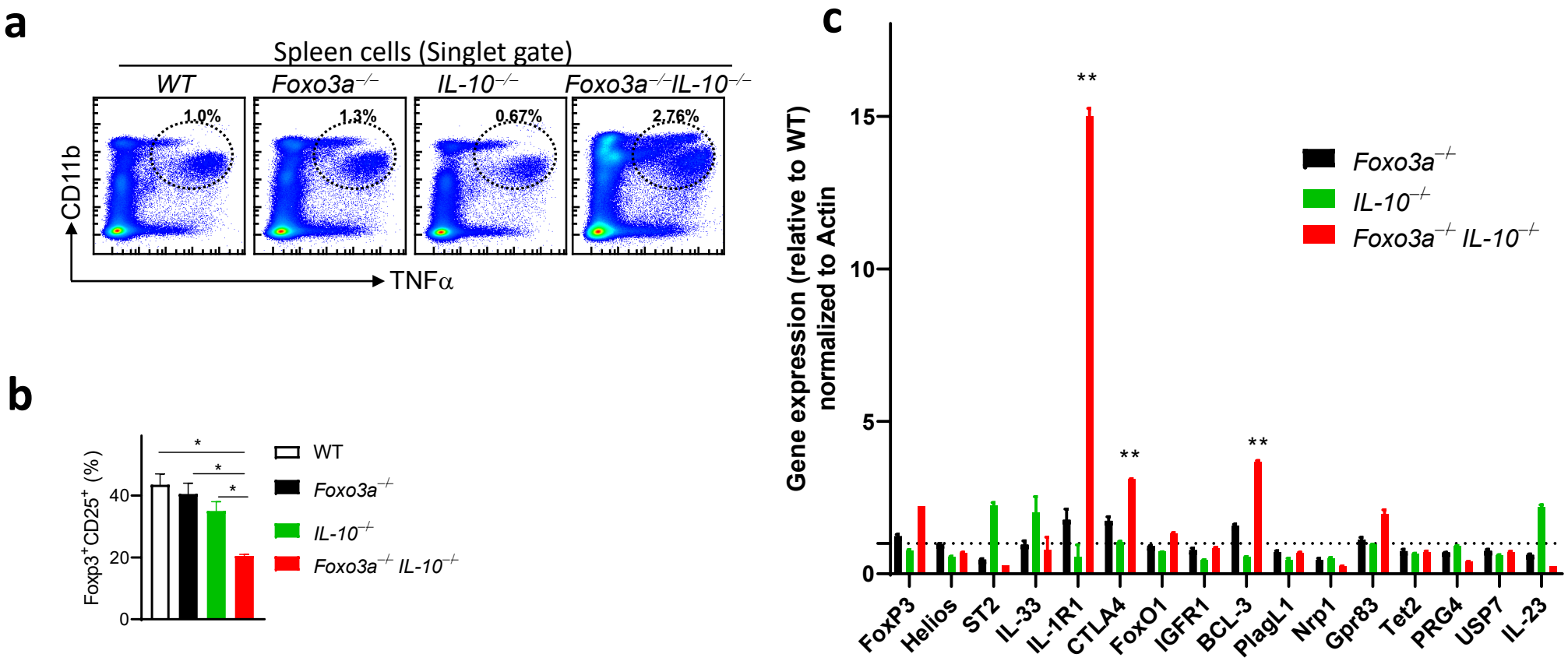

Fig. S4 Foxo3a suppresses a pro-inflammatory response in the absence of IL-10.

(**a**) Representative FACS plots showing TNFα-producing myeloid cells ($CD11b^+$) in the spleens of WT, *Foxo3a*$^{-/-}$, *Il-10*$^{-/-}$ and *Foxo3a*$^{-/-}$*Il-10*$^{-/-}$ mice at 6 h post-LPS stimulation. (**b**) Quantitation of data shown in Fig. 4 e. (**c**) Expression of various transcripts involved in T-reg function measured (by qRT-PCR) in purified $CD25^+CD4^+$ T cells activated with anti- CD3/CD28 in the presence of rIL-2/$rTGF_\beta$ for 72 h.

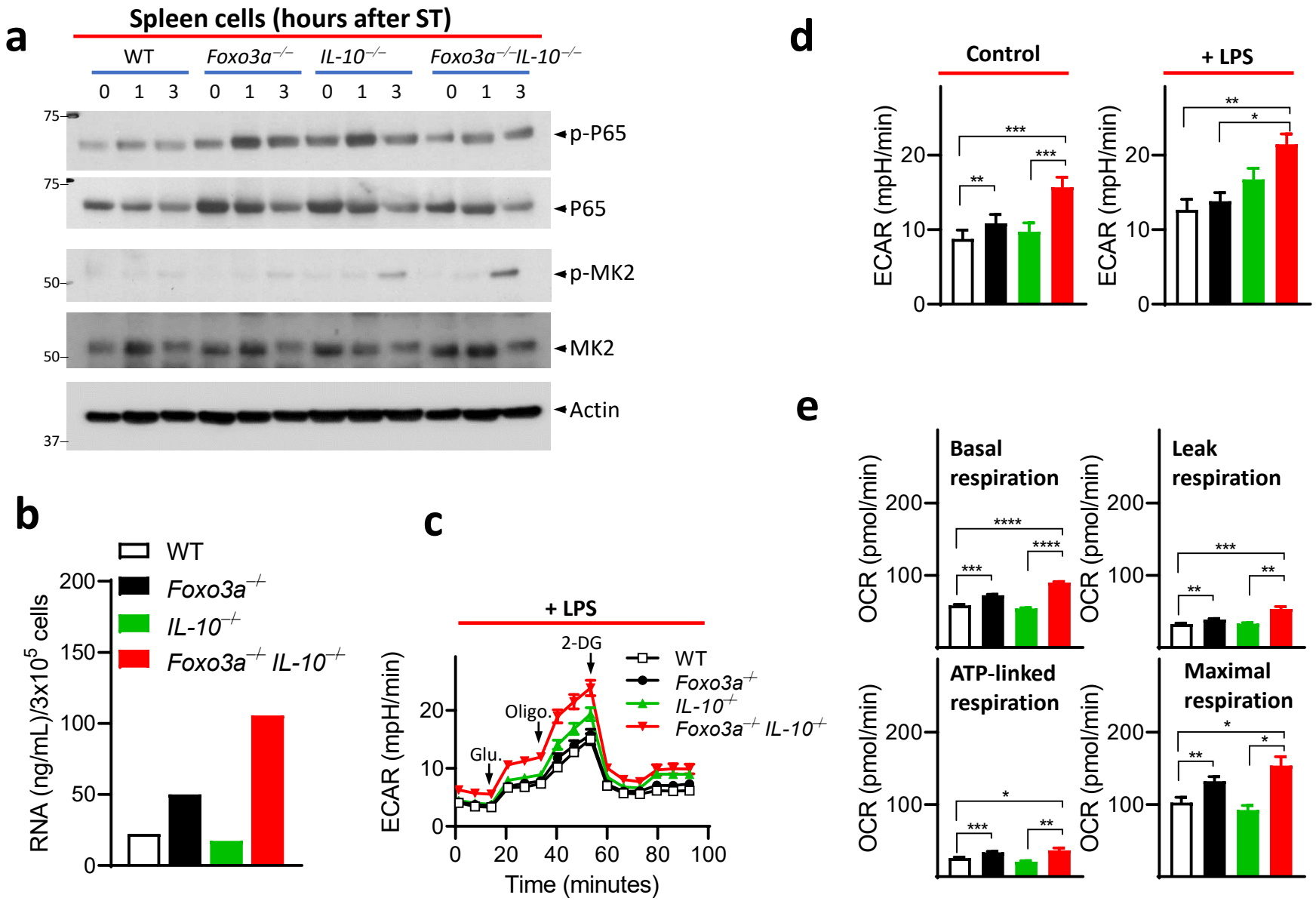

Fig. S5 Deficiency in *Foxo3a* and *Il-10* impacts bioenergetics in spleen cells of mice.

(**a**) Western blots of spleen cell extracts collected at various time intervals post-infection with ST in the four groups of mice. (**b**) RNA amounts measured in $CD4^+$ $CD25^+$ T-cell extracts of the four groups at 72h post-activation with anti-CD3/CD28 and rIL-2/rTGFβ. (**c, d**) ECAR measured in spleen cells of the four groups of mice in the absence and presence of LPS 100 ng/mL. (**e**) Basal respiration, leak respiration, ATP-linked and maximal respiration measured in control spleen cells of the four groups of mice. All graphs depict mean ±SEM. Statistics were done using One-way ANOVA (**P*< 0.05, ****P*<0.001 and *****P*<0.0001).

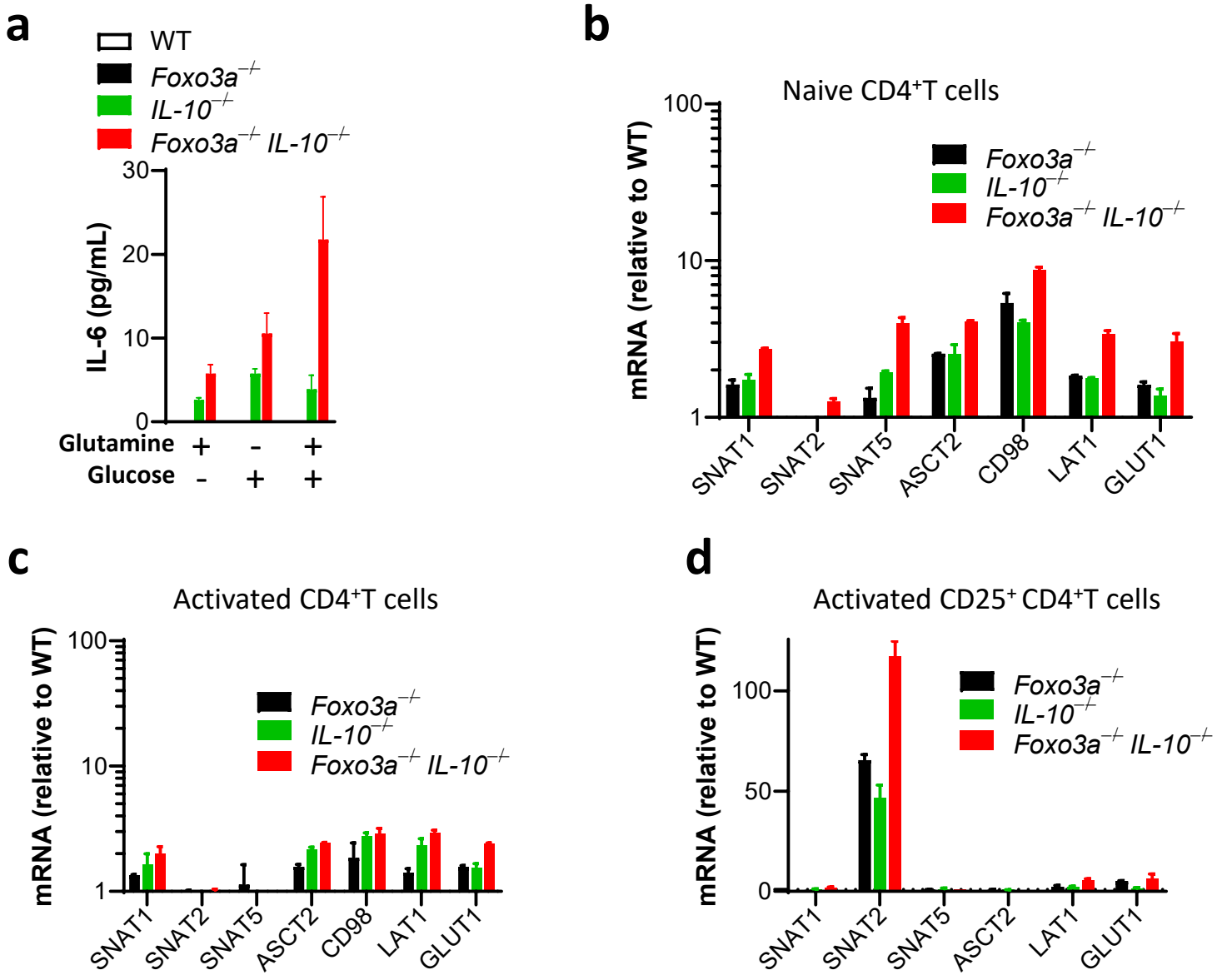

Fig. S6 Modulation of glutamine transporters by Foxo3a and IL-10.

(**a**) IL-6 levels were measured (at 24h) in the supernatants of anti-CD3/CD28 activated $CD4^+$ T-cells supplemented with either 10 mM glucose or 2mM glutamine or both. (**b**) mRNA expression of various glutamine and glucose transporters in non-activated splenic $CD4^+$ T-cells normalized to actin. (**c**) mRNA expression of various glutamine and glucose transporters in anti-CD3/CD28 activated splenic $CD4^+$ T-cells at 48h post activation normalized to actin. (**d**). mRNA expression of various glutamine and glucose transporters in anti-CD3/CD28 activated splenic $CD25^+CD4^+$ T-cells at 72h post activation normalized to actin.

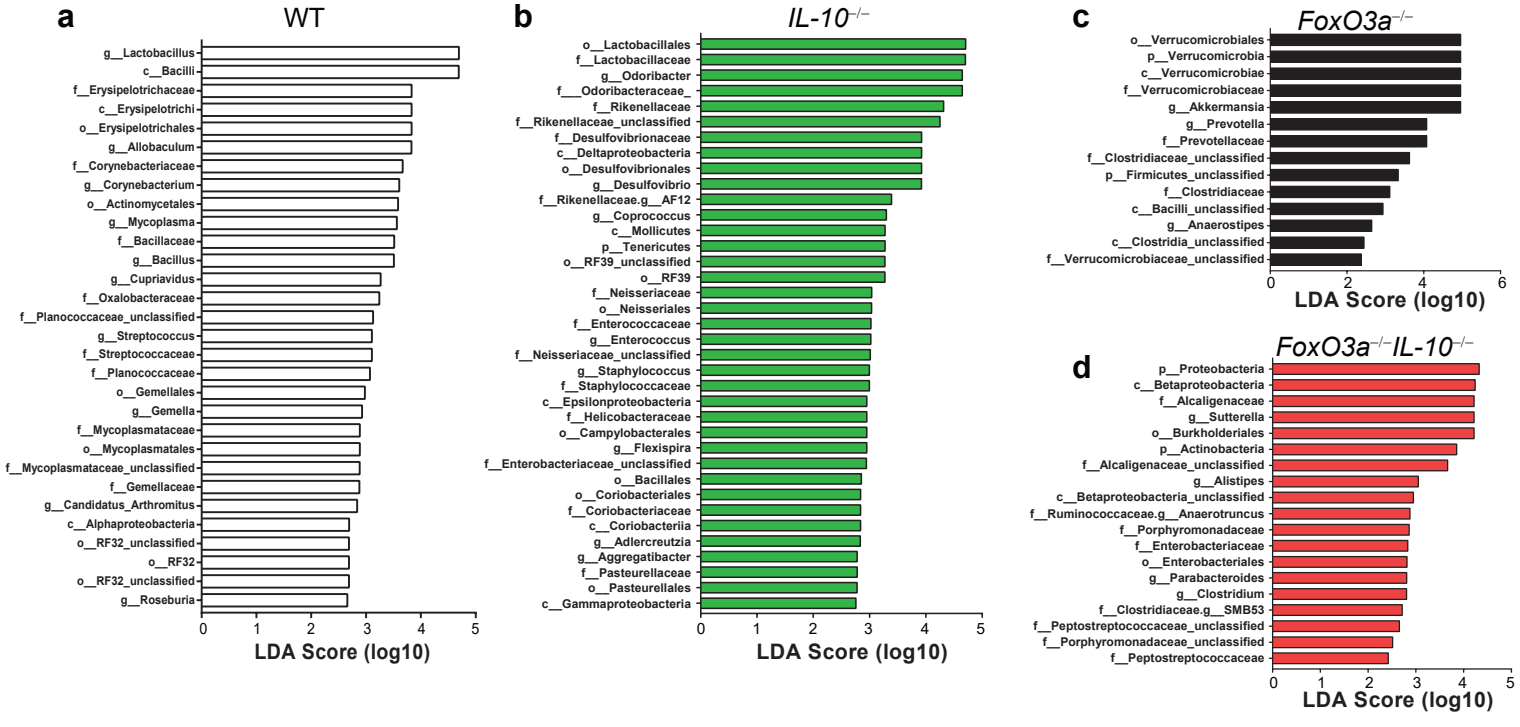

Fig. S7. Microbial taxa that vary significantly in abundance between WT, *Foxo3a*$^{-/-}$, *IL-10*$^{-/-}$, and *Foxo3a*$^{-/-}$*IL-10*$^{-/-}$ mice. Histogram of linear discriminant analysis effect size score of bacterial taxa that are uniquely and significantly enriched in the gut microbiota of each genotype relative to other groups of mice (n=10 each).